Eur. Phys. J. D (2017) 71: 338
DOI: 10.1140/epjd/e2017-80357-5

THE EUROPEAN PHYSICAL JOURNAL D

Regular Article

A moving three-level Λ-type atom in a dissipative cavity

Abdel-Shafy F. Obada[1], Mohamed M.A. Ahmed[1], Ahmed M. Farouk[1,a], and Ahmed Salah[2]

[1] Department of Mathematics, Faculty of Science, Al-Azhar University, Nasr City 11884, Cairo, Egypt
[2] Mathematics and Theoretical Physics Department, Nuclear Research Center, Atomic Energy Authority, Cairo, Egypt

Received 28 May 2017 / Received in final form 18 July 2017
Published online 19 December 2017 –

Abstract. In this paper, we consider a three-level Λ-type atom interacting with a two-mode of electromagnetic cavity field surrounded by a nonlinear Kerr-like medium, the atom and the field are suffering decay rates (i.e. the cavity is not ideal) when the multi-photon processes is considered. Also, the atom and the field are assumed to be coupled with a modulated time-dependent coupling parameter under the rotating wave approximation. The wave function and the probability amplitudes are obtained, when the atom initially prepared in the superposition states and the field initially in the coherent states, by solving the time-dependent Schrödinger equation by taking a proper approximation to the system of differential equations. An analytical expression of the atomic reduced density operator is given. We studied the degree of entanglement, between the field and atom, measure (DEM) via the concurrence, Shannon information entropy, momentum increment and diffusion, and finally we investigated the effects of decay rates and the time-dependent parameters on Husimi Q-function.

1 Introduction

Information cannot be separated from being represented physically. It always be stored in an appropriate physical system and some physical processes can manipulate with it. Quantum entanglement is considered as one of the key resources for quantum information science such as quantum computation and communication [1] and quantum teleportation [2]. Whilst the realization of a quantum computer is along term goal, these pursuits are motivating an enormous amount of cross-disciplinary collaboration in questioning some of the fundamentals of quantum mechanics, information theory, and how the two are related [3]. Since the early days of quantum mechanics, physicists have been puzzled by the counter-intuitive consequences of entanglement [4], which has in fact stimulated an intense debate regarding fundamental issues of quantum theory [5,6]. Recently, a particular attention has been given to develop different methods of entanglement measures [7]. Progress has also been made theoretically in the understanding of quantum entanglement in continuous spaces between two or more modes [8]. The Jaynes-Cummings model (JCM), as is well-known, is a fully quantum mechanical and exactly solvable model which gives a pattern for the description of the most basic and important interaction between light (a single-mode quantized electromagnetic field) and matter (a two-level atom) in the rotating wave approximation (RWA) [9]. The JCM has been the subject of intensive theoretical studies and also of experimental investigations [10,11]. The influence of the external classical field on the entanglement of a two-level atom is studied [12,13] as well as studying the entanglement for a dissipative cavity problem [14–16].

In the recent years, a great attention is paid for studying the interaction between a three-level atom and electromagnetic cavity field. It is important to point out that the increased insight into the dynamics of the three-level systems may be helpful in developing quantum information theory [17–22]. It was demonstrated that key distributions based on three-level quantum systems are more secure against eavesdropping than those based on two-level systems [23,24]. Studying the purity of a three-level atomic system in the presence of Stark shift contributions and the effects of gravity field are presented in [25,26]. The dynamics of entanglement of a three-level atom in motion interacting one and two coupled modes has been investigated [27–30]. Studying the entanglement of a multi-photon three-level atom near the edge of a photonic band gap is presented in [31]. The entanglement between the three-level atom for different configurations and a cavity field (correlated and non-correlated) in the presence of nonlinearities (intensity-dependent coupling and cross and non-linear Kerr medium) is well studied in many cases for initial states of the system [32–38] as well as when the atom and the field are assumed to be coupled with modulated coupling parameter which depends explicitly on time [39]. The autocorrelation function of the light emitted by a microcavity containing a semiconductor quantum well in the non-stationary regime is investigated [40]. Information dynamics of a three-level atom interacting with a damped cavity field is recently investigated taking into consideration that the optical cavity is coupled

[a] e-mail: ahmed.farouk@azhar.edu.eg

to the environment [41]. The effects of an environment on a cavity QED system controlled by bichromatic adiabatic passage is studied for the two-level atomic subsystem [42]. The motion of a pair of solitons propagating through an absorbing three-level atoms in the lambda configuration is analyzed [43]. The transient gain in a three-level system has common features with Dicke super-radiance and can yield strong extreme ultraviolet lasing in, for example He atoms is showed [44]. The optomechanical entanglement of a superconducting charge qubit coupled to a transmission line resonator and a nanomechanical oscillator is studied [45]. The case of a dissipative cavity is studied for a three-level atomic system through master equation methods [46,47] and postulating a non-Hermitian model Hamiltonian [48–50].

This paper is organized as follows: In Section 2, we present a non-Hermitian model Hamiltonian and derive the wave function by using the time-dependent Schrödinger function, solving the system of differential equations and the atomic reduced density matrix is given. In Section 3, we study the Shannon entropy. In Section 4, we study the degree of entanglement by using the concurrence. In Section 5, we study the evolution of Husimi Q-function. In Section 6, we study the atomic momentum increment and momentum diffusion. A conclusion of the paper is presented in Section 7. Finally, we added an appendix shows some detailed mathematical procedure.

2 The physical model

The Hamiltonian $\hat{H}$ specifies the energy levels and time evolution of a quantum theory. A standard axiom of quantum mechanics requires that H be Hermitian because Hermiticity guarantees that the energy spectrum is real and that time evolution is unitary. Hamiltonians that are non-Hermitian have traditionally been used to describe dissipative processes, such as the phenomenon of radioactive decay. However, these non-Hermitian Hamiltonians are only approximate, phenomenological descriptions of physical processes. They cannot be regarded as fundamental because they violate the requirement of unitarity. A non-Hermitian Hamiltonian whose purpose is to describe a particle that undergoes radioactive decay predicts that the probability of finding the particle gradually decreases in time. Of course, a particle cannot just disappear because this would violate the conservation of probability; rather, the particle transforms into other particles. Thus, a non-Hermitian Hamiltonian that describes radioactive decay can at best be a simplified, phenomenological, and non-fundamental description of the decay process because it ignores the precise nature of the decay products [51].

The physical system to be considered is a two-mode field interacting with a three-level Λ-type atom (illustrated schematically in Fig. 1). The non-degenerate case of the quantized radiation field with interaction in the RWA in a non-ideal cavity filled with a Kerr-like medium is assumed. The atom can pass the cavity through a hole. Kerr effect can be observed by surrounding the atom by a nonlinear medium inside a low Q-cavity. To include damping effects, we propose the following non-Hermitian Hamiltonian to describe the moving three-level atom of the Λ-type through the leaking cavity ($\hbar = 1$)

$$\begin{aligned}\hat{H} = {} & \frac{\vec{\hat{p}}^2}{2\mu} + \sum_{\ell=1}^{2} \Omega_\ell \hat{a}_\ell^\dagger \hat{a}_\ell + \sum_{j=1}^{3} \omega_j \hat{\sigma}_{jj} \\ & + \chi \left[\hat{a}_1^\dagger \hat{a}_1 \hat{a}_2^\dagger \hat{a}_2 + \sum_{\ell=1}^{2} \hat{a}_\ell^\dagger \hat{a}_\ell (\hat{a}_\ell^\dagger \hat{a}_\ell - 1) \right] \\ & - i\frac{\bar{\gamma}}{2}\hat{\sigma}_{11} - i\frac{\bar{\Gamma}}{2}(\hat{n}_1 + \hat{n}_2) \\ & + \lambda_1(t)\left(\hat{a}_1^m e^{im\vec{\kappa}_1.\vec{r}}\hat{\sigma}_{12} + \hat{a}_1^{\dagger m} e^{-im\vec{\kappa}_1.\vec{r}}\hat{\sigma}_{21}\right) \\ & + \lambda_2(t)\left(\hat{a}_2^m e^{im\vec{\kappa}_2.\vec{r}}\hat{\sigma}_{13} + \hat{a}_2^{\dagger m} e^{-im\vec{\kappa}_2.\vec{r}}\hat{\sigma}_{31}\right) \end{aligned} \quad (1)$$

where $\hat{p}$ is the momentum operator, μ is the mass of the atom, $\hat{a}_\ell$ ($\hat{a}_\ell^\dagger$) ($\ell = 1, 2$) are the annihilation (creation) operators for the photon field mode under consideration with frequencies Ω_ℓ and they satisfy the commutation relation $[\hat{a}_\ell, \hat{a}_k^\dagger] = \delta_{\ell k}$. $\hat{\sigma}_{ij} = |i\rangle\langle j|$ $(i, j = 1, 2, 3)$ the atomic flip operator for $|j\rangle \to |i\rangle$ transition between the atomic states with energies ω_j and the operators satisfy the commutation relation

$$\left[\hat{\sigma}_{ij}, \hat{\sigma}_{\alpha\beta}\right] = \hat{\sigma}_{i\beta}\delta_{\alpha j} - \hat{\sigma}_{\alpha j}\delta_{i\beta}.$$

Also, $\lambda_\ell(t)$ ($\ell = 1, 2.$) are the coupling parameters between the field and atom where we consider it to be a time-dependent parameters and it may take the form $\lambda_\ell(t) = \bar{\lambda}_\ell \cos(\epsilon t)$ where $\bar{\lambda}_\ell$ is an arbitrary constant and ϵ is the coupling variation parameter. m is the multi-photon parameter. χ denotes the dispersive part of the third-order nonlinearity of the Kerr-like medium, a similar technique has been demonstrated experimentally which the two lasers are coupled through a gas of ^{87}Rb where the photons interact with a Λ-type three-level system [52]. $\bar{\gamma}$ and $\bar{\Gamma}$ are the decaying rates in both the atom and field, respectively, where we consider that the atomic level $|1\rangle$ is decaying with a rate $\bar{\gamma}$ and the electromagnetic field modes are dissipating with a rate $\bar{\Gamma}$ through the cavity. $\vec{\kappa}_\ell$ is the propagation vectors, and $\vec{r}$ is the position vector and they satisfy the following relations [53].

$$\begin{aligned} \left[e^{\pm i\vec{\kappa}_\ell.\vec{r}}, \vec{\hat{p}}\right] &= \mp\vec{\kappa}_\ell e^{\pm i\vec{\kappa}_\ell.\vec{r}}, \\ e^{\pm i\vec{\kappa}_\ell.\vec{r}}|\vec{p}_0\rangle &= |\vec{p}_0 \pm \vec{\kappa}_\ell\rangle, \\ \vec{\hat{p}}\,|\vec{p}_0\rangle &= \vec{p}_0\,|\vec{p}_0\rangle. \end{aligned}$$

Let us now consider the wave function $|\Psi(t)\rangle$ corresponding to the system at any time $t > 0$ to be in the form

$$\begin{aligned} |\Psi(t)\rangle = \sum_{n_1=0}^{+\infty}\sum_{n_2=0}^{+\infty} \big[& A_1(n_1, n_2, t)e^{-i\gamma_1 t}|1; \vec{p}_0; n_1; n_2\rangle \\ & + A_2(n_1, n_2, t)e^{-i\gamma_2 t}|2; \vec{p}_0 - m\vec{\kappa}_1; n_1 + m; n_2\rangle \\ & + A_3(n_1, n_2, t)e^{-i\gamma_3 t}|3; \vec{p}_0 - m\vec{\kappa}_2; n_1; n_2 + m\rangle\big], \end{aligned} \quad (2)$$

where A_1, A_2 and A_3 are the time-dependent probability amplitudes that have to be evaluated, and

$$\gamma_1 = \frac{|\vec{p}_0|^2}{2\mu} + \omega_1 + \Omega_1 n_1 + \Omega_2 n_2,$$
$$\gamma_2 = \frac{|\vec{p}_0 - m\vec{\kappa}_1|^2}{2\mu} + \omega_2 + \Omega_1(n_1 + m) + \Omega_2 n_2,$$
$$\gamma_3 = \frac{|\vec{p}_0 - m\vec{\kappa}_2|^2}{2\mu} + \omega_3 + \Omega_1 n_1 + \Omega_2(n_2 + m). \quad (3)$$

By using the time-dependent Schrödinger equation $i\frac{\partial}{\partial t}|\Psi(t)\rangle = \hat{H}|\Psi(t)\rangle$, we get the following coupled system of differential equations:

$$\dot{A}_1(t) = \nu_1 A_1(t) + \tilde{g}_1 e^{i\Delta_1 t} A_2(t) + \tilde{g}_2 e^{i\Delta_2 t} A_3(t),$$
$$i\dot{A}_2(t) = \tilde{g}_1 e^{-i\Delta_1 t} A_1(t) + \nu_2 A_2(t),$$
$$i\dot{A}_3(t) = \tilde{g}_2 e^{-i\Delta_2 t} A_1(t) + \nu_3 A_3(t),$$

where Δ_1 and Δ_2 are special detuning parameters written in terms of Doppler shift parameter $\frac{\vec{p}_0.\vec{\kappa}_\ell}{\mu}$ and the recoil energy $\frac{m^2\kappa_\ell^2}{2\mu}$ such that

$$\Delta_1 = \omega_1 - \omega_2 - m\Omega_1 + \frac{m^2\kappa_1^2}{2\mu} - \frac{\vec{p}_0.\vec{\kappa}_1}{\mu},$$
$$\Delta_2 = \omega_1 - \omega_3 - m\Omega_2 + \frac{m^2\kappa_2^2}{2\mu} - \frac{\vec{p}_0.\vec{\kappa}_2}{\mu}, \quad (4)$$

$$\tilde{g}_\ell = \bar{\lambda}_\ell \cos(\epsilon t)\sqrt{\frac{(n_\ell + m)!}{n_\ell!}},$$

$$\nu_1 = \chi[n_1 n_2 + n_1(n_1 - 1) + n_2(n_2 - 1)] - i\frac{\bar{\gamma}}{2} - i\frac{\bar{\Gamma}}{2}[n_1 + n_2],$$
$$\nu_2 = \chi[(n_1 + m)n_2 + (n_1 + m)(n_1 + m - 1) + n_2(n_2 - 1)] - i\frac{\bar{\Gamma}}{2}[(n_1 + m) + n_2],$$
$$\nu_3 = \chi[n_1(n_2 + m) + n_1(n_1 - 1) + (n_2 + m)(n_2 + m - 1)] - i\frac{\bar{\Gamma}}{2}[n_1 + (n_2 + m)]. \quad (5)$$

The trigonometric function in $\tilde{g}_\ell$ can be written in an exponential form. We note that there are two exponential terms in the differential equations $e^{\pm i(\Delta_{1,2}+\epsilon)t}$ and $e^{\pm i(\Delta_{1,2}-\epsilon)t}$. As an approximation we neglect the rapidly oscillating (counter rotating) terms $e^{\pm i(\Delta_{1,2}+\epsilon)t}$. This approximation is quite similar to the RWA and has been used extensively to solve such physical models e.g. [54]. So, the system of differential equations can be written as

$$i\dot{A}_1(t) = \nu_1 A_1(t) + \digamma_1 e^{i(\Delta_1-\epsilon)t} A_2(t) + \digamma_2 e^{i(\Delta_2-\epsilon)t} A_3(t),$$
$$i\dot{A}_2(t) = \digamma_1 e^{-i(\Delta_1-\epsilon)t} A_1(t) + \nu_2 A_2(t),$$
$$i\dot{A}_3(t) = \digamma_2 e^{-i(\Delta_2-\epsilon)t} A_1(t) + \nu_3 A_3(t), \quad (6)$$

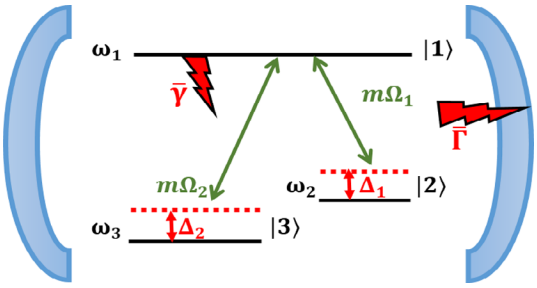

Fig. 1. Schematic diagram of a three-level Λ-type atom with frequencies ω_j $(j = 1, 2, 3)$ interacting with two-mode electromagnetic field with frequencies Ω_ℓ $(\ell = 1, 2)$ in a cavity suffers a decay rates $\bar{\gamma}$ and $\bar{\Gamma}$ for atom and field, respectively.

where the parameter $\digamma_\ell$ after the previous approximation be equal to $\frac{1}{2}\bar{\lambda}_\ell\sqrt{\frac{(n_\ell+m)!}{n_\ell!}}$. By considering the atom to be initially prepared in the superposition of states and the field to be initially prepared in the coherent states $|\alpha_\ell\rangle$ that correspond to a minimum uncertainty state whose center oscillates classically in a harmonic well and retain its shape, where

$$|\alpha_\ell\rangle = \sum_{n_\ell=0}^{+\infty} q_{n_\ell}|n_\ell\rangle, \quad q_{n_\ell} = \exp\left(-\frac{|\alpha_\ell|^2}{2}\right)\frac{\alpha_\ell^{n_\ell}}{\sqrt{n_\ell!}}$$

where q_{n_ℓ} describes the amplitude of the state $|n_\ell\rangle$ of the field mode ℓ and $\bar{n}_\ell = |\alpha_\ell|^2$ denote the mean photon number (intensity of light) of mode ℓ. So, the initial probability amplitudes of the system can be assumed to be $A_1(0) = q_{n_1}q_{n_2}\cos\theta\cos\phi$, $A_2(0) = q_{n_1}q_{n_2}\cos\theta\sin\phi$ and $A_3(0) = q_{n_1}q_{n_2}\sin\theta$. Where θ and ϕ are arbitrary constants that determines the state of the atom i.e. if $\theta = \phi = 0$ we get the excited state, $\theta = \phi = \frac{\pi}{2}$ we get the ground state. When $0 < \theta \leq \pi$ and $0 < \phi \leq \pi$ the atom be initially in the superposition of states.

The system in equation (6) can be solved by the help of Laplace transform after taking the following transformation

$$A_1(t) = B_1(t), \quad A_2(t) = B_2(t)e^{-i(\Delta_1-\epsilon)t},$$
$$A_3(t) = B_3(t)e^{-i(\Delta_2-\epsilon)t}. \quad (7)$$

where $B_j(t)$is an arbitrary function to be determined. After some lengthy but straightforward procedure, the probability amplitudes can be calculated as

$$A_1(t) = i\sum_{j=1}^{3}\frac{\Phi_1^+\Phi_1^- - \mu_j\left(\Phi_1^+ + \Phi_1^-\right) - \mu_j^2}{(\mu_j - \mu_i)(\mu_j - \mu_k)}e^{\mu_j t},$$
$$A_2(t) = -e^{i(\Delta_1-\epsilon)t}\sum_{j=1}^{3}\frac{\Phi_2^+\Phi_2^- - \mu_j\left(\Phi_2^+ + \Phi_2^-\right) - \mu_j^2}{(\mu_j - \mu_i)(\mu_j - \mu_k)}e^{\mu_j t},$$
$$A_3(t) = -e^{i(\Delta_2-\epsilon)t}\sum_{j=1}^{3}\frac{\Phi_3^+\Phi_3^- - \mu_j\left(\Phi_3^+ + \Phi_3^-\right) - \mu_j^2}{(\mu_j - \mu_i)(\mu_j - \mu_k)}e^{\mu_j t} \quad (8)$$

where

$$\Phi_j^{\pm} = \frac{-b_j \pm \sqrt{b_j^2 - 4a_j c_j}}{2a_j}, \tag{9}$$

and

$$\mu_j = -\frac{\mathbb{R}_1}{3} + \frac{2}{3}\sqrt{\mathbb{R}_1^2 - 3\mathbb{R}_2}\cos\left(\delta + \frac{2\pi}{3}(j-1)\right),$$
$$\delta = \frac{1}{3}\cos^{-1}\left(\frac{9\mathbb{R}_1\mathbb{R}_2 - 3\mathbb{R}_1^2 - 27\mathbb{R}_3}{2\left(\mathbb{R}_1^2 - 3\mathbb{R}_2\right)^{3/2}}\right), \tag{10}$$

s.t. the suffixes i, j and $k \in \{1,2,3\}$, and $i \neq j \neq k$.

$$\begin{aligned} a_1 &= -iq_{n_1}q_{n_2}\cos(\theta)\cos(\phi), \\ a_2 &= -q_{n_1}q_{n_2}\cos(\theta)\sin(\phi), \\ a_3 &= -q_{n_1}q_{n_2}\sin(\theta), \end{aligned} \tag{11}$$

$$\begin{aligned} b_1 &= q_{n_1}q_{n_2}\cos(\theta)\cos(\phi)\left(\nu_2+\nu_3-\Delta_1-\Delta_2+2\epsilon\right) \\ &\quad +q_{n_1}q_{n_2}F_2\sin(\theta) - q_{n_1}q_{n_2}F_1\cos(\theta)\sin(\phi), \\ b_2 &= i\cos(\theta)\cos(\phi)[q_{n_1}q_{n_2}F_1 \\ &\quad -q_{n_1}q_{n_2}\tan(\phi)(\nu_1+\nu_3-\Delta_2+\epsilon)], \\ b_3 &= iq_{n_1}q_{n_2}F_2\cos(\theta)\cos(\phi) \\ &\quad -iq_{n_1}q_{n_2}\sin(\theta)(\nu_1+\nu_2-\Delta_1-\epsilon), \end{aligned} \tag{12}$$

$$\begin{aligned} c_1 &= iq_{n_1}q_{n_2}\cos(\theta)\cos(\phi)\left(\nu_3-\Delta_2+\epsilon\right)\left(\nu_2-\Delta_1+\epsilon\right) \\ &\quad -iq_{n_1}q_{n_2}F_1\cos(\theta)\sin(\phi)\left(\nu_3-\Delta_2+\epsilon\right) \\ &\quad -iq_{n_1}q_{n_2}F_2\sin(\theta)(\nu_2-\Delta_1+\epsilon), \\ c_2 &= -\cos(\theta)\{q_{n_1}q_{n_2}\sin(\phi)[F_2^2-\nu_1(\nu_3-\Delta_2+\epsilon)] \\ &\quad +q_{n_1}q_{n_2}F_1\cos(\phi)(\nu_3-\Delta_2+\epsilon)\} \\ &\quad +q_{n_1}q_{n_2}F_1F_2\sin(\theta), \\ c_3 &= -q_{n_1}q_{n_2}\sin(\theta)[F_1^2-\nu_1(\nu_2-\Delta_1+\epsilon)] \\ &\quad +F_2\cos(\theta)\{q_{n_1}q_{n_2}F_1\sin(\phi) \\ &\quad -q_{n_1}q_{n_2}\cos(\phi)(\nu_2-\Delta_1+\epsilon)\}, \end{aligned} \tag{13}$$

and

$$\begin{aligned} \mathbb{R}_1 &= i(\nu_1+\nu_2\nu_3-\Delta_1-\Delta_2+2\epsilon), \\ \mathbb{R}_2 &= F_1^2+F_2^2-\nu_1(\nu_2+\nu_3)+\nu_2\nu_3 \\ &\quad +\Delta_1(\nu_1+\nu_3-\Delta_2+\epsilon) \\ &\quad +\Delta_2(\nu_1+\nu_2+\epsilon)-\epsilon(\epsilon+2\nu_1+\nu_2+\nu_3), \\ \mathbb{R}_3 &= iF_2^2(\nu_2-\Delta_1+\epsilon)+i(\nu_3-\Delta_2+\epsilon) \\ &\quad \times\{F_1^2-\nu_1(\nu_2-\Delta_1+\epsilon)\}. \end{aligned} \tag{14}$$

The reduced density operator of the atom $\hat{\rho}_A(t)$ is given by

$$\hat{\rho}_A(t) = Tr_F\left(|\Psi(t)\rangle\langle\Psi(t)|\right) = \begin{pmatrix} \varrho_{11} & \varrho_{12} & \varrho_{13} \\ \varrho_{21} & \varrho_{22} & \varrho_{23} \\ \varrho_{31} & \varrho_{32} & \varrho_{33} \end{pmatrix} \tag{15}$$

where the elements of this matrix are:

$$\varrho_{jj}(t) = \sum_{n_1=0}^{+\infty}\sum_{n_2=0}^{+\infty} A_j(n_1,n_2,t)A_j^*(n_1,n_2,t), \quad j=1,2,3. \tag{16}$$

$$\begin{aligned} \varrho_{12}(t) &= e^{-i\Delta_1 t}e^{im\vec{\kappa}_1.\vec{r}} \\ &\quad \times\sum_{n_1=0}^{+\infty}\sum_{n_2=0}^{+\infty} A_1(n_1+m,n_2,t)A_2^*(n_1,n_2,t) \\ &= \varrho_{21}^*(t), \end{aligned} \tag{17}$$

$$\begin{aligned} \varrho_{13}(t) &= e^{-i\Delta_2 t}e^{im\vec{\kappa}_2.\vec{r}} \\ &\quad \times\sum_{n_1=0}^{+\infty}\sum_{n_2=0}^{+\infty} A_1(n_1,n_2+m,t)A_3^*(n_1,n_2,t) \\ &= \varrho_{31}^*(t), \end{aligned} \tag{18}$$

$$\begin{aligned} \varrho_{23}(t) &= e^{i(\Delta_1-\Delta_2)t}e^{im(\vec{\kappa}_2-\vec{\kappa}_1).\vec{r}} \\ &\quad \times\sum_{n_1=0}^{+\infty}\sum_{n_2=0}^{+\infty} A_2(n_1,n_2+m,t)A_3^*(n_1,n_2+m,t) \\ &= \varrho_{32}^*(t). \end{aligned} \tag{19}$$

The reduced density operator of the field $\hat{\rho}_F(t)$ is given by

$$\hat{\rho}_F(t) = Tr_A\left(|\Psi(t)\rangle\langle\Psi(t)|\right). \tag{20}$$

Once the density matrix and the wave function are obtained, we can discuss different physical phenomena. In all next numerical calculations we set the value of $m = 1$ i.e. the *one-photon* transition. Many authors have studied the multi-photon transition in JC-model for example [55]. Some of experiments that demonstrates the quantum behavior of light in an undergraduate laboratory has been described in [56]. There are many physical situations where such models may find applications [57] and [58]. Moreover it is worthwhile to remark that investigating such models goes beyond an intrinsic theoretical interest in condensed matter systems too, because the development of new and improved materials is expected to lead to the fabrication of three dimensional photonic band gap systems possessing few isolated high-Q resonant field modes [59]. It is worth mentioning that two-photon transitions may occur, for example, in atom-field diamagnetic interactions. It has been shown that such transitions contribute in dispersion interactions in lower-order perturbative calculations [60] when compared to the single-photon transitions. The process of non-degenerate two-photon transition can be physically demonstrated via making an atomic transition from the ground (excited)

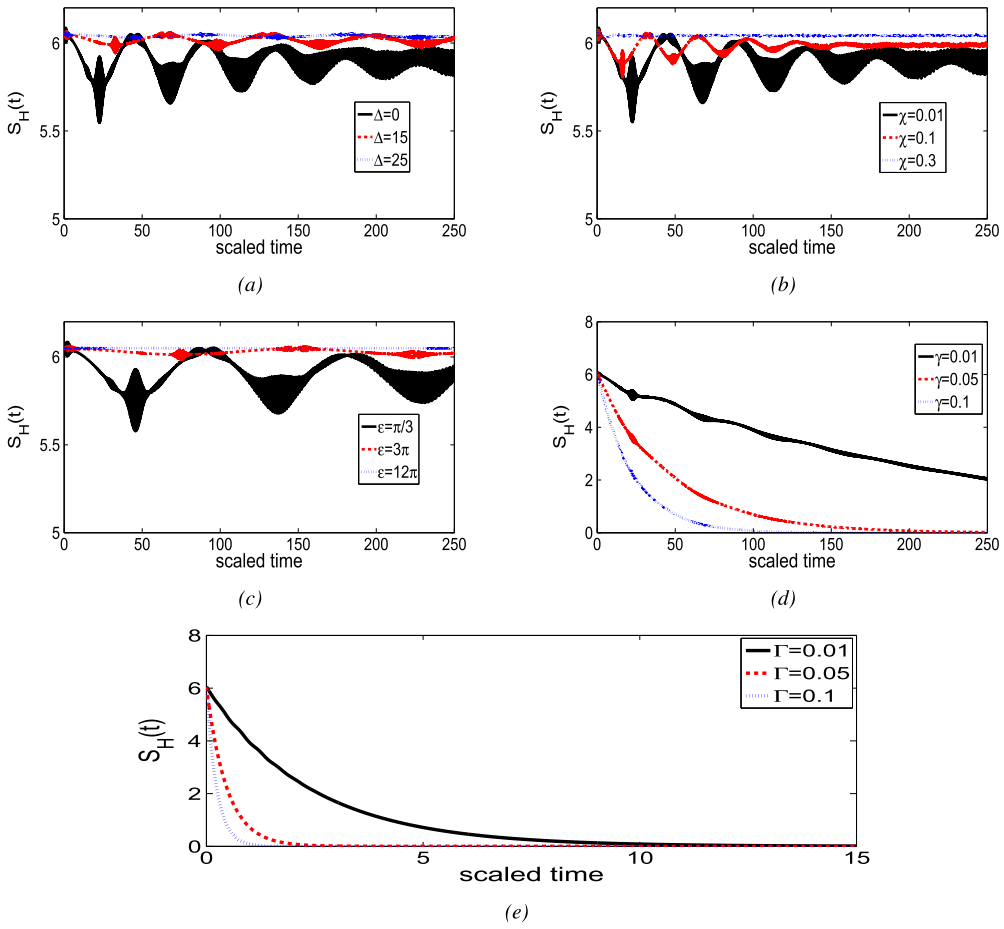

Fig. 2. The evolution of Shannon entropy $S_H(t)$ vs. the scaled time $\bar{\lambda}t$ with $\bar{n}_\ell = 25$, $\ell = 1, 2$, $\Delta_1 = \Delta_2 = \Delta$, $\theta = \phi = 0$ and $m = 1$ (one-photon process).

state to an excited (ground) state by simultaneously absorbing (emitting) two laser photons. Particularly, in the case of two-photon absorption, the atom first absorbs one photon and jumps from a *real* level to a higher *virtual* one, and then by the absorption of a second photon jumps to the nearest *real* level.

3 Shannon entropy

Shannon's entropy has played an important role in the study of quantum-mechanical systems and clarifying some fundamental concepts. In an analogous way, Shannon information entropy corresponding to the photon number distribution [61]. Shannon information is defined to solve the problem of the most efficient coding of a set of signals. In the context of probability distribution, it is defined as

$$S_H(t) = -\sum_{n_1=0}^{+\infty}\sum_{n_2=0}^{+\infty} \ln\left\{\mathcal{P}(\mathrm{n_1},\mathrm{n_2},\mathrm{t})^{\mathcal{P}(\mathrm{n_1},\mathrm{n_2},\mathrm{t})}\right\} \qquad (21)$$

where

$$\mathcal{P}(n_1, n_2, t) = \langle n_1, n_2|\, \hat{\rho}_F\, |n_1, n_2\rangle$$

which is the photon number distribution, where $\hat{\rho}_F$ is the field reduced density operator for the considered system. Therefore, we can state that

$$\mathcal{P}(n_1, n_2, t) = [|A_1(n_1, n_2, t)|^2 + |A_2(n_1 + m, n_2, t)|^2 + |A_3(n_1, n_2 + m, t)|^2]. \qquad (22)$$

It is noted that the Shannon information entropy for photon number operator is given by using the diagonal elements of density operator and contains no phase information, but it provides some useful information about the behavior of photon number distribution (i.e., entropy is the amount of random information in a system).

In Figure 2, we plot the results obtained numerically by considering the atom to be initially prepared in the upper most state (i.e. $\theta = 0$, $\phi = 0$) and the to be initially in the coherent states. Generally, we note that the upper bound of $S_H(t)$ here is 6.1 and by comparing this result with [6,62], we may conclude that the upper bound of Shannon entropy is related to the initial number of photons $\bar{n}$ by the relation $S_{\mathrm{Max}} \leq \ln(\bar{n})$ s.t. $\bar{n} > 1$. In Figure 2a we set three different values of the detuning parameter $\Delta_1 = \Delta_2 = \Delta$ and fixed all other parameters to be zero i.e. $\chi = 0$, $\epsilon = 0$ and $\bar{\gamma} = \bar{\Gamma} = 0$. We note here that in the absence of Δ,

the entropy has an envelope oscillation as the interaction time goes on and the envelope oscillation is periodic. By considering the presence of a detuning parameter Δ, we note that entropy increases, collapse time increases, the oscillation is squeezed and periodicity decreased. In Figure 2b, we set three different values of the third-order non-linearity of the Kerr-like medium and fixed all other parameters to be zero i.e. $\Delta = 0$, $\epsilon = 0$ and $\bar{\gamma} = \bar{\Gamma} = 0$. We note that the small value of χ as shown in the black-solid curve of Figure 2b by comparing it with the black-solid curve of Figure 2a, there is no change in the oscillation of Shannon entropy. But for large values of χ, we note that entropy increases, collapse time decreases and the periodicity increases. So, the high-value of χ affected on $S_H(t)$ to be sustainable for along time, in its high degree. In Figure 2c, we set three different values of the parameter ϵ that controls the variation of the coupling parameter $\lambda(t)$ and fixed all other parameters to equal zero i.e. $\chi = 0$, $\Delta = 0$ and $\bar{\gamma} = \bar{\Gamma} = 0$. We note that the collapse time in the presence of the parameter ϵ is increased to be more than the collapse time in the case of $\epsilon = 0$. In Figure 2d, we set three different values of the atomic damping factor $\bar{\gamma}$ and fixed all other parameters to be zero i.e. $\chi = 0$, $\epsilon = 0$ and $\Delta = 0$. We note that for a weak damping factor the entropy decreases and for larger values of $\bar{\gamma}$ we note that entropy is pulled down rapidly to reach zero. In Figure 2e, we set three values of the field damping factor $\bar{\Gamma}$. We note that the general behavior of Shannon entropy is similar to the case of atom-damping but it takes much less interaction time to reach zero entropy compared with atomic case.

4 Concurrence

Despite the fact that the possibility of quantum entanglement, between the field and atom, was acknowledged almost as soon as quantum theory was discovered [4], it is only in the last few decades that consideration has been given to finding mathematical methods to quantify entanglement. The first point to note is that no measure of entanglement can be linear in the system state. This follows directly from the fact that entanglement be invariant under local unitary transformations. In the case of pure quantum states for two subsystems, a number of physically intuitive measures of entanglement have been known for some time, however for general mixed states of an arbitrary number of subsystems, entanglement measures are still under development. Several measures are proposed to quantify the degree of entanglement (DEM) [63]. The DEM is investigated by using von Neumann entropy for a three-level atomic system with arbitrary forms of non-linearity is studied in [34,35].

The concurrence is presented by Hill and Wootters [64,65] as a suitable measure of entanglement of any state of two qubits, mixed or pure. For a pure state $|\Psi(t)\rangle$ on $(M \times N)$-dimensional Hilbert space $\mathcal{R} = \mathcal{R}_M \bigotimes \mathcal{R}_N$. The concurrence can be defined as [66]

$$\mathcal{C}(t) = \sqrt{2\Big(|\langle\Psi(t)|\Psi(t)\rangle|^2 - Tr\left(\rho_N^2(t)\right)\Big)} \qquad (23)$$

such that $\hat{\rho}_N(t) = Tr_M\left(|\Psi(t)\rangle\langle\Psi(t)|\right)$ is the reduced density operator of the subsystem with dimension N and Tr_M is the partial trace over $\mathcal{R}_M$. The concurrence as a measure of entanglement degree ensures the scale between 0 for a separable (disentangled) state and $\sqrt{2(N-1)/N}$ for the maximally entangled state, and monotonically increases as entanglement grows. To investigate the concurrence we calculated the atomic reduced density matrix in (15), so we can rewrite concurrence in the following form

$$\mathcal{C}(t) = \sqrt{2\sum_{i,j=1,2,3,i\neq j}\Big(\varrho_{ii}\varrho_{jj} - \varrho_{ij}\varrho_{ji}\Big)}. \qquad (24)$$

In Figure 3, we plot the evolution of concurrence $\mathcal{C}(t)$ vs. the scaled time $\bar{\lambda}t$ when $\bar{n}_\ell = 25$, $(\ell = 1, 2)$. In Figure 3a, we set three different values of the detuning parameter Δ and fixed all other parameters to zero i.e. $\chi = 0$, $\epsilon = 0$ and $\bar{\gamma} = \bar{\Gamma} = 0$. We note that when $\Delta = 0$, black-solid line, the oscillation of the envelope curve is periodic and as time goes on the lower points of the concurrence goes up and by taking into account the presence of the detuning parameter we note that the almost stable period increased and the periodicity decreased and the DEM is pulled down as Δ increases. So, The detuning parameter makes the atom-field interaction weak. In Figure 3b, we take into account the presence of Kerr medium parameter χ and fixed all other parameters to be equal zero i.e. $\Delta = 0$, $\epsilon = 0$ and $\bar{\gamma} = \bar{\Gamma} = 0$. We note that for a small effect of χ, the stable period of DEM, increases and revival times spread wide as time goes on. While by increasing the value of χ the periodicity increases and DEM is pulled down. In Figure 3c, we set three different values of ϵ that controls the time dependence of the atom-field coupling function and fixed all other parameters to be equal zero i.e. $\chi = 0$, $\Delta = 0$ and $\bar{\gamma} = \bar{\Gamma} = 0$. We note that its effect is increasing the collapse time to be doubled compared by the case where we ignore ϵ (black-solid line in Fig. 3a). As the value of ϵ grows up, the collapse time increases and the DEM decreases. In Figures 3d and 3e, we study and compare the behavior of DEM evolution of the considered system where atom and the field are suffering decay rates $\bar{\gamma}$ and $\bar{\Gamma}$, respectively. We note that the disentangled state (death of entanglement) in different periods and it is obvious that the disentangled state is reached much rapidly for the field dissipation more than the case of the atomic decay.

In Figure 4, we plot the concurrence $\mathcal{C}(\bar{n})$ vs. the mean photon number (intensity of light) $\bar{n} = |\alpha|^2$, at a certain time-point $\bar{\lambda}t = \frac{\pi}{4}$. Generally, we note that concurrence decreases as $\bar{n}$ grows and the effect of χ, $\bar{\gamma}$ and $\bar{\Gamma}$ on the concurrence not change the initial value (when $\bar{n} = 0$) of the concurrence. In Figure 4b, we noticed that when $C \cong 0.58$, there is a reverse relation between the initial number of photons and the value of Kerr parameter, that would help us to control the degree of entanglement. In Figure 4d, we set three different values of the atomic decay rate $\bar{\gamma}$ and we note that the relation between concurrence and the mean photon number is not affected by $\bar{\gamma}$. However it decreases sharply by increasing t as shown in Figure 4e.

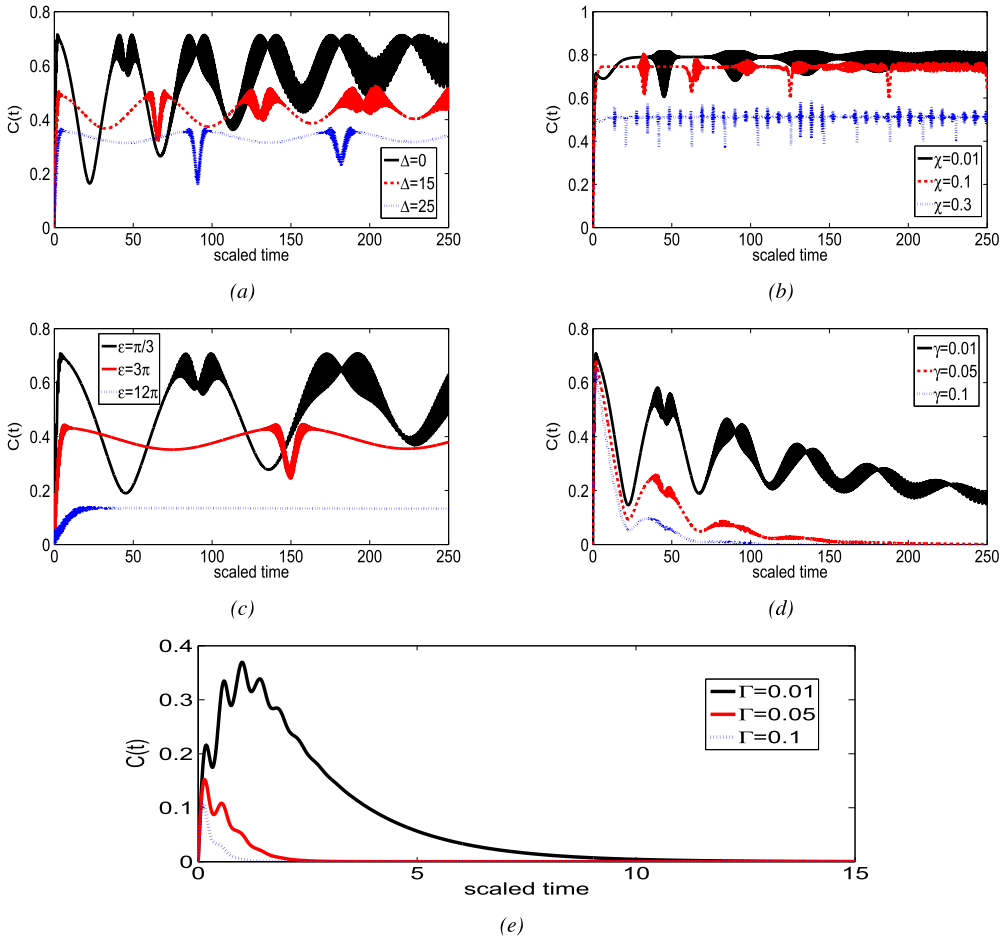

Fig. 3. The evolution of concurrence $\mathcal{C}(t)$ vs. the scaled time $\bar{\lambda}t$ with $\bar{n}_\ell = 25$, $\ell = 1, 2$, $\Delta_1 = \Delta_2 = \Delta$, $\theta = \phi = 0$ and $m = 1$ (one-photon process).

Generally, we note that the best degree of entanglement is obtained when the atom-field interaction is surrounded by a weak non-linear Kerr like medium as we see in Figure 3b the curves of concurrence are sustainable and be near to its maximal when $\chi = 0.01$ or 0.1, while the degree of entanglement decreases if χ grows more. This result agrees with [36,67]. We note that in Figure 4b, the best values of concurrence be when $\chi = 0.1$ and that occurs when $\bar{n} = |\alpha|^2 = 10$ and 30.

5 Husimi Q-function

The quasi-probability distribution functions have become a main tool to investigate experimental results in detecting quantum states of systems. These functions can be detected in homodyne experiments [68]. The quasi-probability distribution functions are c-number functions and not necessary to be positive, that allows us to calculate the expectation values of a quantum state. The calculations of quasi-probability distribution functions, given a density matrix, are often a tedious task that involves integration over phase space variables. The Q-function is simply expressed as the coherent expectation value of the reduced field density matrix, so it is widely used to investigate the field dynamics. It has no singularity problems at all. It exists for any density matrix, is bounded and even is greater than or equal to zero. Moreover, the width of the Q-function gives a measure for the light squeezing. Therefore, it is interesting to investigate the behavior of Q-function (Fig. 5). It is defined by [69]

$$Q(\alpha_1, \alpha_2, t) = \frac{1}{\pi^2} \langle \alpha_1, \alpha_2 | \, \hat{\varrho}_F \, | \alpha_1, \alpha_2 \rangle = \frac{1}{\pi^2} \sum_{j=1}^{3} |\psi_j(\alpha_1, \alpha_2, t)|^2, \quad (25)$$

where $\hat{\varrho}_F$ is the reduced field density operator and $|\alpha_\ell\rangle$ is the coherent state defined by

$$|\alpha_\ell\rangle = e^{-\frac{1}{2}|\alpha_\ell|^2} \sum_{n_\ell=0}^{+\infty} \frac{\alpha_\ell^{n_\ell}}{\sqrt{n_\ell!}} |n_\ell\rangle, \quad \alpha_\ell = x_\ell + i y_\ell, \quad (26)$$

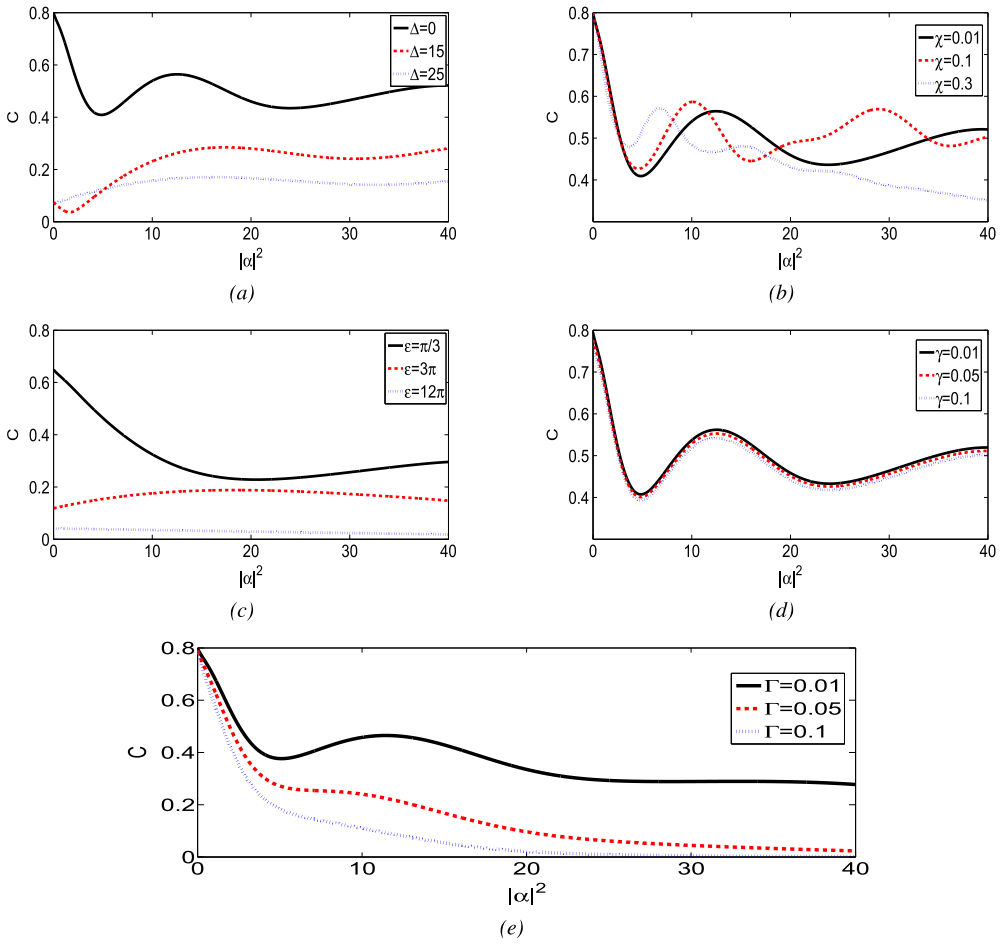

Fig. 4. The evolution of concurrence $\mathcal{C}(\bar{n})$ vs. the mean photon number (intensity of light) $\bar{n}$, $\Delta_1 = \Delta_2 = \Delta$, $\theta = \phi = 0$ and $m = 1$ (one-photon process).

and $\psi_j(\alpha_1, \alpha_2, t)$ are given by

$$\psi_1(\alpha_1,\alpha_2,t) = e^{-\frac{1}{2}(|\alpha_1|^2+|\alpha_2|^2)} \sum_{n_1=0}^{+\infty}\sum_{n_2=0}^{+\infty} q_{n_1} q_{n_2} \times \frac{\alpha_1^{*n_1}}{\sqrt{n_1!}} \frac{\alpha_2^{*n_2}}{\sqrt{n_2!}} A_1(n_1,n_2,t),$$

$$\psi_2(\alpha_1,\alpha_2,t) = e^{-\frac{1}{2}(|\alpha_1|^2+|\alpha_2|^2)} \sum_{n_1=0}^{+\infty}\sum_{n_2=0}^{+\infty} q_{n_1} q_{n_2} \times \frac{\alpha_1^{*n_1+m}}{\sqrt{(n_1+m)!}} \frac{\alpha_2^{*n_2}}{\sqrt{n_2!}} A_2(n_1+m,n_2,t),$$

$$\psi_3(\alpha_1,\alpha_2,t) = e^{-\frac{1}{2}(|\alpha_1|^2+|\alpha_2|^2)} \sum_{n_1=0}^{+\infty}\sum_{n_2=0}^{+\infty} q_{n_1} q_{n_2} \frac{\alpha_1^{*n_1}}{\sqrt{n_1!}} \times \frac{\alpha_2^{*n_2+m}}{\sqrt{(n_2+m)!}} A_3(n_1,n_2+m,t). \quad (27)$$

In Figures 6–9, we sketch the shape of the Husimi Q-function in the subspace $\alpha_1 = \alpha_2 = \alpha$ in the complex α-plane where $x = Re(\alpha)$ and $y = Im(\alpha)$ when the Kerr-like parameter $\chi = 1.0\bar{\lambda}$. It is noted that by applying a strong Kerr medium ($\chi = 1\bar{\lambda}$) to the system, Q-function is split into eight fully-separated peaks, if a quasi-probability distribution function exhibits different peaks around different system variables the system is expected to spend a relatively large amount of time in the vicinity of these variables and a short amount of time between the peaks. In many cases in the context of quantum optics this is linked to multi-stability. Examples of papers where this kind of behavior is studied [70–73]. We take into consideration the effect of the time varying coupling parameter ϵ, the atom and field decay rates $\bar{\gamma}$ and $\bar{\Gamma}$, respectively. In Figure 6, we set three different values of the parameter ϵ, we note that there is no effect on the distribution of Husimi Q-function by the parameter ϵ. Nor the shape and the peak height are changed. In Figure 7, we set three different values for the atom decay rate $\bar{\gamma}$, we note that the shape of Husimi Q function is not changed but the peaks height is decreasing by the growing in the decay rate $\bar{\gamma}$. In Figures 8 and 9, we sketch the 3D and contour plots of Husimi Q-function and we set three different values for the field decay rate $\bar{\Gamma}$. We note that the shape and the peaks height of Husimi Q function are changed. When we set $\bar{\Gamma} = \frac{1}{2}\bar{\lambda}$, we note that the height is decreased from 1.4×10^{-3} (as in Fig. 6a) to 1.2×10^{-10} (as in Fig. 8a) and the contour shape is very slightly changed. By increasing the value of $\bar{\Gamma}$, the peak

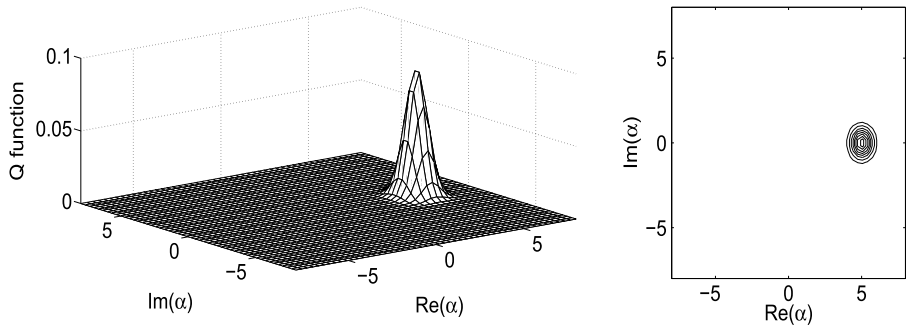

Fig. 5. The sketch of Husimi Q-function in the subspace $\alpha_1 = \alpha_2 = \alpha$ in the complex α-plane when $t = \frac{\pi}{4}\bar{\lambda}$ with $\bar{n}_\ell = 25$, $\ell = 1, 2$, $\chi = 0$, $\Delta = 0$, $\epsilon = 0$, $m = 1$ (one-photon process), $\bar{\gamma} = 0$ and $\bar{\Gamma} = 0$.

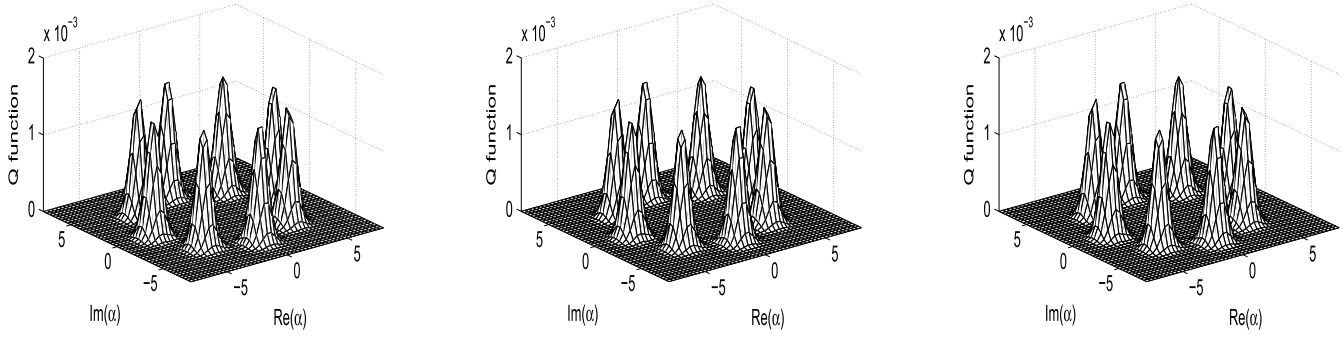

(a) $\epsilon = 0$. *(b)* $\epsilon = \frac{\pi}{3}$. *(c)* $\epsilon = 12\pi$.

Fig. 6. The 3D sketch of Husimi Q-function in the subspace $\alpha_1 = \alpha_2 = \alpha$ in the complex α-plane when $t = \frac{\pi}{4}\bar{\lambda}$ with $\bar{n}_\ell = 25$, $\ell = 1, 2$, $\chi = 1\bar{\lambda}$, $\Delta = 0$, $\theta = \phi = 0$, $\bar{\gamma} = 0$ and $\bar{\Gamma} = 0$.

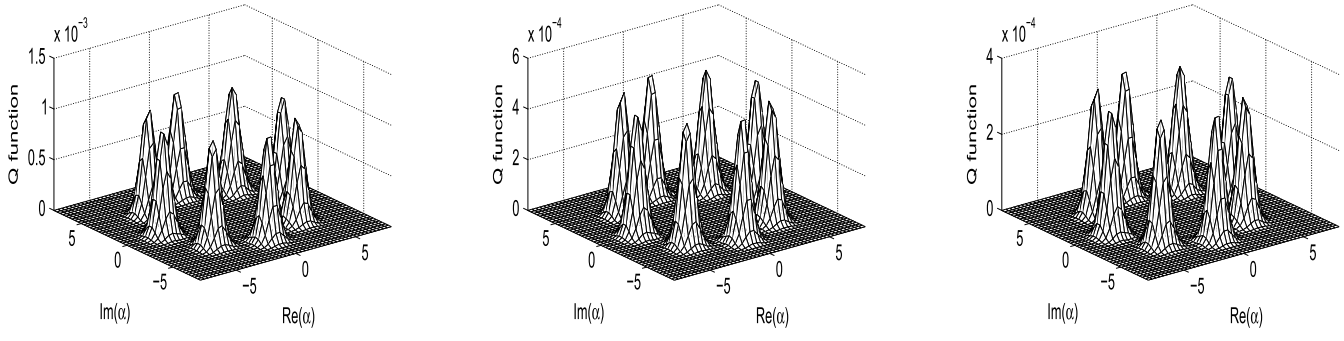

(a) $\bar{\gamma} = \frac{1}{2}\bar{\lambda}$. *(b)* $\bar{\gamma} = \frac{3}{2}\bar{\lambda}$. *(c)* $\bar{\gamma} = 2\bar{\lambda}$.

Fig. 7. The 3D sketch of Husimi Q-function in the subspace $\alpha_1 = \alpha_2 = \alpha$ in the complex α-plane when $t = \frac{\pi}{4}\bar{\lambda}$ with $\bar{n}_\ell = 25$, $\ell = 1, 2$, $\chi = 1\bar{\lambda}$, $\Delta = 0$, $\epsilon = 0$, $\theta = \phi = 0$, $m = 1$ (one-photon process) and $\bar{\Gamma} = 0$.

height decreases and the number of peaks decreases also besides squeezing effect is shown. It decreased from 8 fully-separated peaks to 5 semi-separated peaks in Figures 9b and 9c with squeezing pattern being observed. So, if the system suffers a field decay rate, its stability decreases.

6 Momentum increment and diffusion

Cooling atoms by laser is based on the momentum exchange between the particles and the electromagnetic field via the connection between the photon absorption and emission. Laser cooling is generally limited by the random fluctuations in the exchanged momentum between photons and atoms, that give rise to atomic momentum diffusion. Momentum increment and momentum diffusion are defined respectively as [74]

$$\begin{aligned} \langle(\Delta\vec{p})\rangle &= \langle\vec{p}\rangle - \vec{p}_0, \\ \langle(\Delta\vec{p})^2\rangle &= \langle\vec{p}^2\rangle - \langle\vec{p}\rangle^2. \end{aligned} \tag{28}$$

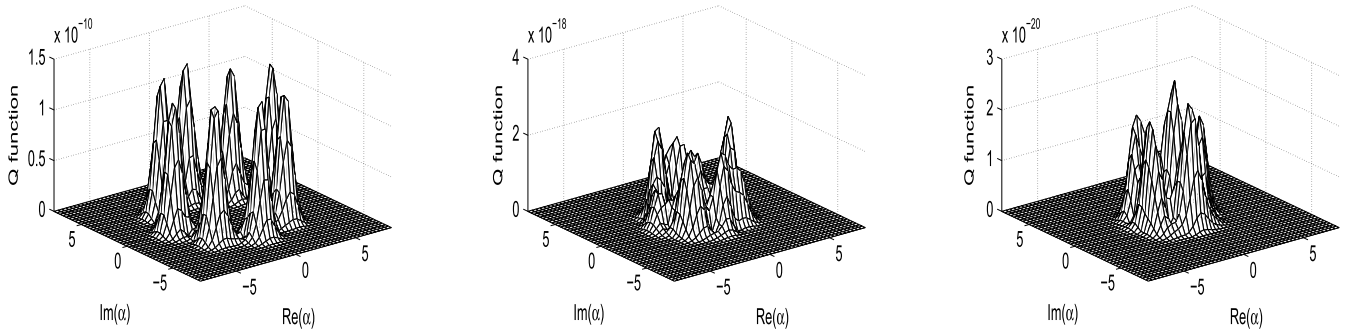

(a) $\bar{\Gamma} = \frac{1}{2}\bar{\lambda}$. *(b)* $\bar{\Gamma} = \frac{3}{2}\bar{\lambda}$. *(c)* $\bar{\Gamma} = 2\bar{\lambda}$.

Fig. 8. The 3D sketch of Husimi Q-function in the subspace $\alpha_1 = \alpha_2 = \alpha$ in the complex α-plane when $t = \frac{\pi}{4}\bar{\lambda}$ with $\bar{n}_\ell = 25$, $\ell = 1, 2$, $\chi = 1\bar{\lambda}$, $\Delta = 0$, $\theta = \phi = 0$, $\epsilon = 0$, $m = 1$ (one-photon process) and $\bar{\gamma} = 0$.

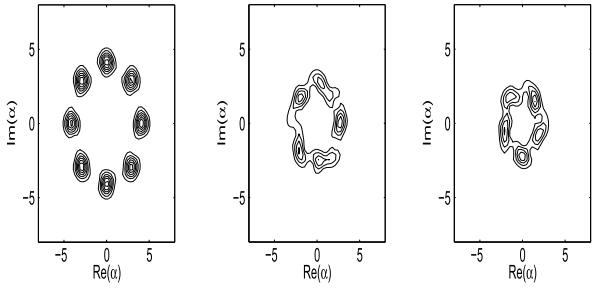

(a) $\bar{\Gamma} = \frac{1}{2}\bar{\lambda}$. *(b)* $\bar{\Gamma} = \frac{3}{2}\bar{\lambda}$. *(c)* $\bar{\Gamma} = 2\bar{\lambda}$.

Fig. 9. The contour plots of Husimi Q-function as in Figure 8.

The expectation values of the momentum increment and momentum diffusion for the considered model, respectively are given by (considering $\vec{\kappa}_1 = \vec{\kappa}_2 = \vec{\kappa}$.)

$$\begin{aligned}\langle(\Delta\vec{p})\rangle &= \vec{p}_0(\varrho_{11}(t) + \varrho_{22}(t) + \varrho_{33}(t) - 1)\\ &\quad -m\vec{\kappa}(\varrho_{22}(t) + \varrho_{33}(t)),\\ \langle(\Delta\vec{p})^2\rangle &= |\vec{p}_0|^2(\varrho_{11}(t) + \varrho_{22}(t) + \varrho_{33}(t))\\ &\quad +|\vec{p}_0 - m\vec{\kappa}|^2(\varrho_{22}(t) + \varrho_{33}(t)) - \langle\vec{p}\rangle^2. \quad (29)\end{aligned}$$

In Figure 10, we plot the evolution of scaled momentum increment $\frac{\langle(\Delta\vec{p})\rangle.\vec{\kappa}}{|\vec{\kappa}|^2}$ (black-dotted curve) and scaled momentum diffusion $\frac{\langle(\Delta\vec{p})^2\rangle}{|\vec{\kappa}|^2}$ (black-solid curve) vs. the scaled time $\bar{\lambda}t$ and we focus only on the effects of the decay rates $\bar{\gamma}$ and $\bar{\Gamma}$ and the parameter ϵ of the time-varying coupling between the atom and field. In Figure 10a, we set all parameters equal to zero and we note that increment base line oscillates around $\frac{-1}{2}$ and the diffusion started from zero as the initial point and doesn't exceed the value $\frac{1}{4}$. In Figures 10b and 10c, we set the atomic decay rate $\bar{\gamma} = 0.01\bar{\lambda}$ and $0.1\bar{\lambda}$, respectively. We note that the rate of diffusion decreased to reach zero after a proper time period which means that momentum exchange between the field and atom is harmed due to the atomic decay rate which is better results from that appear in applying a field decay rate to the system as in Figures 10d and 10e. In Figure 10f, we set $\epsilon = 3\pi$, we note that the diffusion rate decreased and revival times delayed.

7 Results and conclusion

In the previous sections of this paper, we studied the interaction between a moving three-level atom in Λ configuration and a two-mode electromagnetic field in a dissipative cavity, surrounded by a nonlinear Kerr-like medium. We have obtained the form of the corresponding wave function, considering the atom initially in the superposition of states and the field in the coherent state, and solved the time-dependent Schrödinger equation by using Laplace transformations to the coupled system of differential equations after taking a RWA-like approximation. We studied the effects of detuning, Kerr-like medium, the coupling time varying and the decay rates parameters on some non-classical statistical aspects. We studied Shannon information entropy, the DEM through concurrence, Husimi Q-function, momentum increment and diffusion. The results of this paper may be summed as follows:

– The effects of both the detuning parameter Δ and the time-varying coupling parameter ϵ are quite similar. We note that they reduce the DEM, increase the collapse times, reduce the peak-height of Husimi Q-function but preserve its geometrical shape.

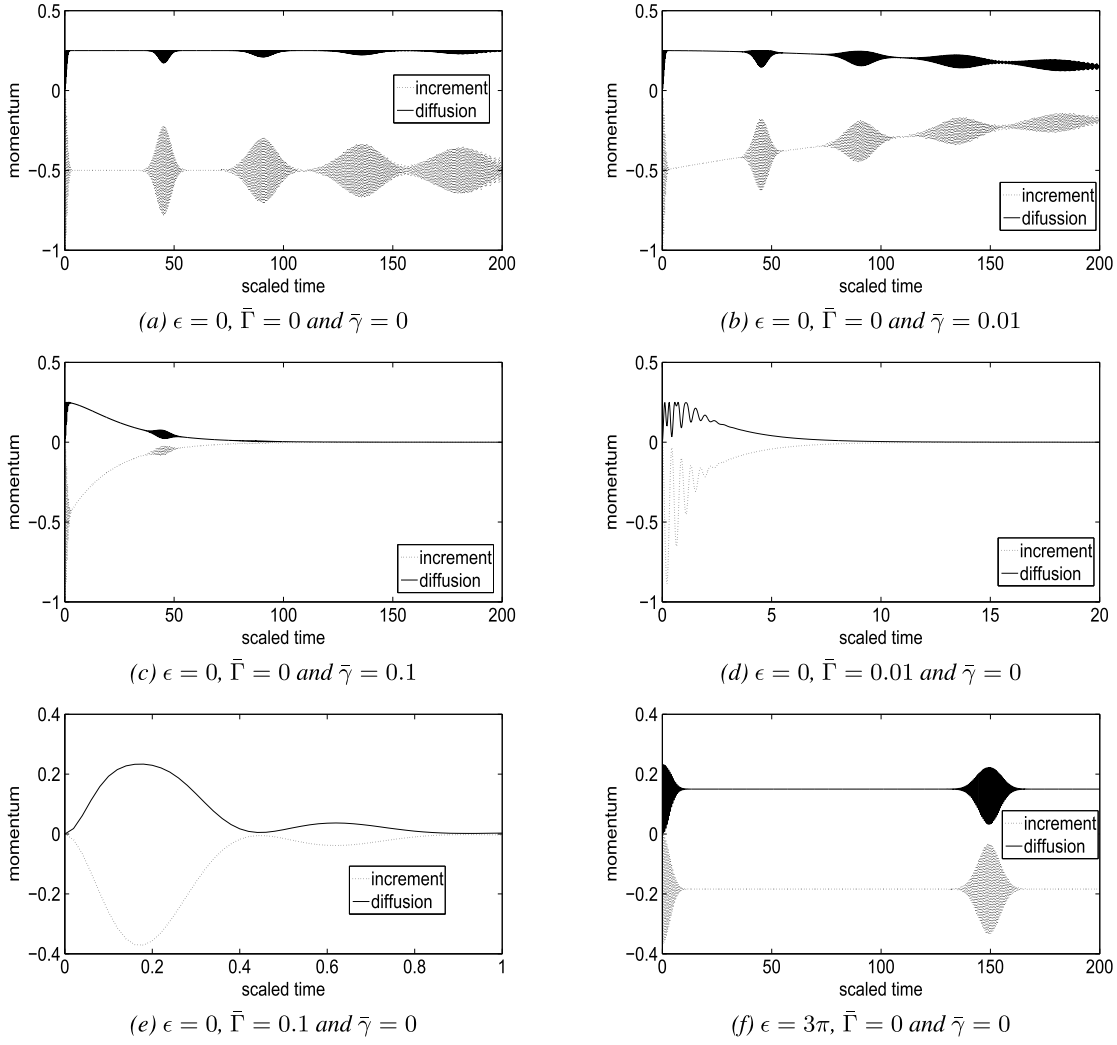

(a) $\epsilon = 0$, $\bar{\Gamma} = 0$ *and* $\bar{\gamma} = 0$ (b) $\epsilon = 0$, $\bar{\Gamma} = 0$ *and* $\bar{\gamma} = 0.01$

(c) $\epsilon = 0$, $\bar{\Gamma} = 0$ *and* $\bar{\gamma} = 0.1$ (d) $\epsilon = 0$, $\bar{\Gamma} = 0.01$ *and* $\bar{\gamma} = 0$

(e) $\epsilon = 0$, $\bar{\Gamma} = 0.1$ *and* $\bar{\gamma} = 0$ (f) $\epsilon = 3\pi$, $\bar{\Gamma} = 0$ *and* $\bar{\gamma} = 0$

Fig. 10. The evolution of scaled momentum increment $\frac{\langle(\Delta\vec{p})\rangle.\vec{\kappa}}{|\vec{\kappa}|^2}$ (black-dotted line) and scaled momentum diffusion $\frac{\langle(\Delta\vec{p})^2\rangle}{|\vec{\kappa}|^2}$ (black-solid line) vs. the scaled time $\bar{\lambda}t$ with $\bar{n}_\ell = 25$, $\ell = 1, 2$, $\theta = \phi = 0$, $\Delta_1 = \Delta_2 = \Delta = 0$, $\chi = 0$, $m = 1$ (one-photon process) and $\vec{p}_0 = \vec{0}$.

– We note that the best degree of entanglement is obtained when the atom-field interaction is surrounded by a weak non-linear Kerr like medium as we see in Figure 3b the curves of concurrence are sustainable and be near to its maximal when $\chi = 0.01$ or 0.1, while the degree of entanglement decreases if χ grows more. This result agrees with [36,67]. We note that in Figure 4b, the best values of concurrence be when $\chi = 0.1$ and that occurs when $\bar{n} = |\alpha|^2 = 10$ and 30.
– In Figure 4b, we noticed that when $C \cong 0.58$, there is a reverse relation between the initial number of photons and the value of Kerr parameter, that would help us to control the degree of entanglement.
– The atomic decay rate $\bar{\gamma}$ is not effective in the evolution of concurrence vs. the mean photon number $\bar{n}$, as in Figure 4d, while it reduces the peak-height of Husimi Q-function but preserves its geometrical shape.
– The effect of the field decay rate $\bar{\Gamma}$ is to bring the DEM to zero more quickly than the effect of $\bar{\gamma}$, it destroys the geometrical shape of Husimi Q-function, which reduces the system stability.
– The sensitivity of entanglement to the field decay is much greater than the atomic decay.
– The upper bound of $S_H(t)$ is 6.1 and by comparing this result with [6,62], we may conclude that the upper bound of Shannon entropy is related to the initial number of photons $\bar{n}$ by the relation $S_{\text{Max}} \leq \ln(\bar{n}) = \sum_{\ell=1}^{\varpi} \ln \bar{n}_\ell$ s.t. $\bar{n}_\ell > 1$ and ϖ is the number of field modes. So, we may reformulate the definition of Shannon information entropy as $\mathbb{S}_{\mathbb{H}}(t) = \frac{1}{\sum_{\ell=1}^{\varpi} \ln \bar{n}_\ell} \ln\left\{\mathcal{P}(n_1, n_2, t)^{\mathcal{P}(n_1,n_2,t)}\right\}$. With this reformulation of the definition we get a bounded evolution between 0 and 1 which may be used as an indicator to the degree of entanglement.

The authors would like to thank the anonymous referees for their objective comments that improved the text in many points.

Author contribution statement

Profs. A.-S.F. Obada and M.M.A. Ahmed supervised the project. Ahmed M. Farouk performed the mathematical analysis, numerical calculations and wrote the manuscript. Ahmed Salah developed the mathematical analysis. All Authors shared equally in discussing the results.

Appendix A

In this Appendix, we show the detailed derivation of the probability amplitudes in equation (8) by using Laplace transformations. The system of differential equations in (6) can written by using equation (7) as:

$$\begin{aligned} i\dot{B}_1(t) &= \nu_1 B_1(t) + \digamma_1 B_2(t) + \digamma_2 B_3(t), \\ i\dot{B}_2(t) &= \digamma_1 B_1(t) + (\nu_2 - \Delta_1 + \epsilon)\, B_2(t), \\ i\dot{B}_3(t) &= \digamma_2 B_1(t) + (\nu_3 - \Delta_2 + \epsilon)\, B_3(t). \end{aligned} \tag{A.1}$$

By introducing Laplace transform of the probability amplitudes $B_j(t)$

$$Y_j(s) = \int_0^\infty dt B_j(t) e^{-st}, \quad j = 1, 2, 3, \tag{A.2}$$

then the differential equations in (A.1) obey the following algebraic system:

$$\begin{aligned} i(sY_1(s) - q_{n_1} q_{n_2} \cos(\theta)\cos(\phi)) &= \nu_1 Y_1(s) + \digamma_1 Y_2(s) \\ &\quad + \digamma_2 Y_3(s), \\ i(sY_2(s) - q_{n_1+m} q_{n_2} \cos(\theta)\sin(\phi)) &= \digamma_1 Y_1(s) + (\nu_2 \\ &\quad - \Delta_1 + \epsilon) Y_2(s), \\ i(sY_3(s) - q_{n_1} q_{n_2+m} \sin(\theta)) &= \digamma_2 Y_1(s) + (\nu_3 \\ &\quad - \Delta_2 + \epsilon) Y_3(s). \end{aligned} \tag{A.3}$$

The solution of the algebraic system is given by

$$\begin{aligned} Y_1(s) &= i\frac{a_1 s^2 + b_1 s + c_1}{s^3 + \mathbb{R}_1 s^2 + \mathbb{R}_2 s + \mathbb{R}_3} \\ &= i\frac{\left(s - \Phi_1^+\right)\left(s - \Phi_1^-\right)}{\left(s - \mu_1\right)\left(s - \mu_2\right)\left(s - \mu_3\right)}, \\ Y_2(s) &= -\frac{a_2 s^2 + b_2 s + c_2}{s^3 + \mathbb{R}_1 s^2 + \mathbb{R}_2 s + \mathbb{R}_3} \\ &= -\frac{\left(s - \Phi_2^+\right)\left(s - \Phi_2^-\right)}{\left(s - \mu_1\right)\left(s - \mu_2\right)\left(s - \mu_3\right)}, \\ Y_3(s) &= -\frac{a_3 s^2 + b_3 s + c_3}{s^3 + \mathbb{R}_1 s^2 + \mathbb{R}_2 s + \mathbb{R}_3} \\ &= -\frac{\left(s - \Phi_3^+\right)\left(s - \Phi_3^-\right)}{\left(s - \mu_1\right)\left(s - \mu_2\right)\left(s - \mu_3\right)}, \end{aligned} \tag{A.4}$$

where $\phi_j^\pm$ and μ_j are defined in equations (9) and (10), respectively. By applying the partial-fraction decomposition method to the last three equations and performing the inverse Laplace transform on the resulting equations, we get the probability amplitudes in equation (8).

References

1. C.H. Bennett, D.P. DiVincenzo, Nature **404**, 247 (2000)
2. C.H. Bennett, G. Brassard, C. Crépeau, R. Jozsa, A. Peres, W.K. Wootters,Phys. Rev. Lett. **70**, 1895 (1993)
3. P. Kok, W.J. Munro, K. Nemoto, T.C. Ralph, J.P. Dowling, G.J. Milburn, Rev. Mod. Phys. **79**, 135 (2007)
4. A. Einstein, B. Podolsky, N. Rosen, Phys. Rev. **47**, 777 (1935)
5. M.N. O'Sullivan-Hale, I.A. Khan, R.W. Boyd, J.C. Howell, Phys. Rev. Lett. **94**, 220501 (2005)
6. M. Abdel-Aty, J. Phys. A: Math. Gen. **38**, 8589 (2005)
7. V. Vedral, M.B. Plenio, M.A. Rippin, P.L. Knight, Phys. Rev. Lett. **78**, 2275 (1997)
8. R.W. Rendell, A.K. Rajagopal, Phys. Rev. A **72**, 012330 (2005)
9. E.T. Jaynes, F.W. Cummings, Proc. IEEE **51**, 89 (1963)
10. B.W. Shore, P.L. Knight, J. Mod. Opt. **40**, 1195 (1993)
11. G. Rempe, H. Walther, N. Klein, Phys. Rev. Lett. **58**, 353 (1987)
12. E.M. Khalil, Int. J. Theor. Phys. **52**, 1122 (2013)
13. M.S. Abdalla, A.-S.F. Obada, E.M. Khalil, Opt. Commun. **285**, 1283 (2012)
14. K. Berrada, S. Abdel-Khalek, A.-S.F. Obada, Phys. Lett. A **376**, 1412 (2012)
15. J.-S. Zhang, J.-B. Xu, Opt. Commun. **282**, 2543 (2009)
16. A. Nourmandipour, M.K. Tavassoly, Eur. Phys. J. Plus **130**, 1 (2015)
17. S.-B. Zheng, Quantum Semiclass. Opt.: J. Eur. Opt. Soc. B **10**, 691 (1998)
18. H.-I. Yoo, J.H. Eberly, Phys. Rep. **118**, 239 (1985)
19. M. Alexanian, S.K. Bose, Phys. Rev. A **52**, 2218 (1995)
20. A.-S.F. Obada, A.M. Abdel-Hafez, J. Mod. Opt. **34**, 665 (1987)
21. M.H. Mahran, A.-R.A. El-Samman, A.-S.F. Obada, J. Mod. Opt. **36**, 53 (1989)
22. A.M. Abdel-Hafez, A.S.F. Obada, M.M.A. Ahmad, Physica A **144**, 530 (1987)
23. N.J. Cerf, M. Bourennane, A. Karlsson, N. Gisin, Phys. Rev. Lett. **88**, 127902 (2002)
24. M. Bourennane, A. Karlsson, G. Björk, Phys. Rev. A **64**, 012306 (2001)
25. A.-S.F. Obada, M.M.A. Ahmed, A. Salah, A.M. Farouk, J. Mod. Opt. **63**, 2315 (2016)
26. N.H. Abd El-Wahab, A.S.A. Rady, A.-N.A. Osman, A. Salah, Eur. Phys. J. Plus **130**, 1 (2015)
27. X. Liu, Physica A **286**, 588 (2000)
28. N.H. Abd El-Wahab, A.S.A. Rady, A.-N.A. Osman, A. Salah, J. Rus. Laser Res. **36**, 423 (2015)
29. M.J. Faghihi, M.K. Tavassoly, M. Hatami, Physica A **407**, 100 (2014)
30. M.J. Faghihi, M.K. Tavassoly, M.R. Hooshmandasl, JOSA B **30**, 1109 (2013)
31. M. Abdel-Aty, Laser Phys. **16**, 1381 (2006)
32. M. Ghorbani, H. Safari, M.J. Faghihi, JOSA B **33**, 1022 (2016)
33. M.J. Faghihi, M.K. Tavassoly, JOSA B **30**, 2810 (2013)

34. A.-S.F. Obada, S.A. Hanoura, A.A. Eied, Laser Phys. **24**, 055201 (2014)
35. A.-S.F. Obada, S.A. Hanoura, A.A. Eied, Laser Phys. **23**, 055201 (2013)
36. A.-S.F. Obada, A.A. Eied, Opt. Commun. **282**, 2184 (2009)
37. A.-S.F. Obada, M. Abdel-Aty, Physica A **329**, 53 (2003)
38. A.-S.F. Obada, S.A. Hanoura, A.-H. Eied, Eur. Phys. J. D **68**, 18 (2014)
39. N.H. Abd El-Wahab, A. Salah, A.S.A. Rady, A.-N.A. Osman, Differ. Equ. Dyn. Syst. (2016), DOI: 10.1007/s12591-016-0291-0
40. H. Eleuch, Int. J. Mod. Phys. B **24**, 5653 (2010)
41. A.-B.A. Mohamed, H. Eleuch, Eur. Phys. J. Plus **132**, 75 (2017)
42. H. Eleuch, S. Guerin, H.R. Jauslin, Phys. Rev. A **85**, 1 (2012)
43. H. Eleuch, R. Bennaceur, J. Opt. A: Pure Appl. Opt. **5**, 528 (2003)
44. E.A. Sete, A.A. Svidzinsky, Y.V. Rostovtsev, H. Eleuch, P.K. Jha, S. Suckewer, M.O. Scully, IEEE J. Sel. Top. Quantum Electron. **18**, 541 (2012)
45. E.A. Sete, H. Eleuch, Phys. Rev. A **89**, 1 (2014)
46. H.J. Carmichael, D.F. Walls, J. Phys. B: At. Mol. Phys. **9**, 1199 (1976)
47. S. Abdel-Khalek, K. Berrada, M.R.B. Wahiddin, J. Comput. Theor. Nanosci. **12**, 3970 (2015)
48. W.B. Cardoso, A.T. Avelar, B. Baseia, Physica A **388**, 1331 (2009)
49. G.-F. Zhang, X.-C. Xie, Eur. Phys. J. D **60**, 423 (2010)
50. R. Daneshmand, M.K. Tavassoly, Eur. Phys. J. D **70**, 101 (2016)
51. C.M. Bender, Rep. Prog. Phys. **70**, 947 (2007)
52. A. Sinatra, J.-F. Roch, K. Vigneron, P. Grelu, J.-Ph. Poizat, K. Wang, P. Grangier, Phys. Rev. A **57**, 2980 (1998)
53. W.H. Louisell, *Quantum statistical properties of radiation* (Wiley, New York, 1973)
54. W.H. Louisell, A. Yariv, A.E. Siegman, Phys. Rev. **124**, 1646 (1961)
55. M. Kozierowski, S.M. Chumakov, J.J. Sanchez-Mondragon, J. Mod. Opt. **40**, 1763 (1993)
56. J.J. Thorn, M.S. Neel, V.W. Donato, G.S. Bergreen, R.E. Davies, M. Beck, Am. J. Phys. **72**, 1210 (2004)
57. J.D. Andersen, V.M. Kenkre, Phys. Rev. B **47**, 11134 (1993)
58. Y. Yamamoto, S. Machida, G. Björk, Opt. Quantum Electron. **24**, S215 (1992)
59. Y. Yamamoto, R.E. Slusher, *Optical processes in microcavities* (Springer US, Boston, MA, 1995)
60. S.Y. Buhmann, H. Safari, S. Scheel, A. Salam, Phys. Rev. A **87**, 012507 (2013)
61. C.E. Shannon, *The mathematical theory of communication* (University of Illinois Press, Urbana, 1949)
62. S.J.D. Phoenix, P.L. Knight, Ann. Phys. **186**, 381 (1988)
63. M. Abdel-Aty, Prog. Quantum Electron. **31**, 1 (2007)
64. S. Hill, W.K. Wootters, Phys. Rev. Lett. **78**, 5022 (1997)
65. W.K. Wootters, Phys. Rev. Lett. **80**, 2245 (1998)
66. R. Horodecki, P. Horodecki, M. Horodecki, K. Horodecki, Rev. Mod. Phys. **81**, 865 (2009)
67. M. Abdel-Aty, Laser Phys. **11**, 871 (2001)
68. U. Leonhardt, *Measuring the quantum state of light* (Cambridge University Press, New York, 1997)
69. R.J. Glauber, Phys. Rev. **131**, 2766 (1963)
70. K. Vogel, H. Risken, Phys. Rev. A **39**, 4675 (1989)
71. H.J. Carmichael, Phys. Rev. X **5**, 1 (2015)
72. W. Casteels, R. Fazio, C. Ciuti, Phys. Rev. A **95**, 1 (2017)
73. J.M. Fink, A. Dombi, A. Vukics, A. Wallraff, P. Domokos, Phys. Rev. X **7** 1 (2017)
74. N.H. Abdel-Wahab, Phys. Scr. **71**, 132 (2005)